Disruption of P450-mediated vitamin E hydroxylase activities alters vitamin E status in tocopherol supplemented mice and reveals extra-hepatic vitamin E metabolism

Sabrina A. Bardowell,* Xinxin Ding,[†,§] and Robert S. Parker[1,*]

[1]Division of Nutritional Sciences,* Cornell University, Ithaca, NY; Wadsworth Center,[†] New York State Department of Health, Albany, NY; and School of Public Health,[§] State University of New York, New York, NY

Abstract **The widely conserved preferential accumulation of α-tocopherol (α-TOH) in tissues occurs, in part, from selective postabsorptive catabolism of non-α-TOH forms via the vitamin E-ω-oxidation pathway. We previously showed that global disruption of CYP4F14, the major but not the only mouse TOH-ω-hydroxylase, resulted in hyper-accumulation of γ-TOH in mice fed a soybean oil diet. In the current study, supplementation of *Cyp4f14*$^{-/-}$ mice with high levels of δ- and γ-TOH exacerbated tissue enrichment of these forms of vitamin E. However, at high dietary levels of TOH, mechanisms other than ω-hydroxylation dominate in resisting diet-induced accumulation of non-α-TOH. These include TOH metabolism via ω-1/ω-2 oxidation and fecal elimination of unmetabolized TOH. The ω-1 and ω-2 fecal metabolites of γ- and α-TOH were observed in human fecal material. Mice lacking all liver microsomal CYP activity due to disruption of cytochrome P450 reductase revealed the presence of extra-hepatic ω-, ω-1, and ω-2 TOH hydroxylase activities. TOH-ω-hydroxylase activity was exhibited by microsomes from mouse and human small intestine; murine activity was entirely due to CYP4F14. These findings shed new light on the role of TOH-ω-hydroxylase activity and other mechanisms in resisting diet-induced accumulation of tissue TOH and further characterize vitamin E metabolism in mice and humans.**—Bardowell, S. A., X. Ding, and R. S. Parker. **Disruption of P450-mediated vitamin E hydroxylase activities alters vitamin E status in tocopherol supplemented mice and reveals extra-hepatic vitamin E metabolism. *J. Lipid Res.* 2012.** 53: **2667–2676.**

Supplementary key words ω-oxidation • CYP4F14 • CYP4F2 • cytochrome P450 reductase • knockout mouse • liver • intestine • fecal elimination • diet • metabolites

Vitamin E, a family of plant-derived lipophilic compounds that consists of tocopherols (TOH) and tocotrienols (T3), is considered to be the most important group of lipophilic antioxidants. These structurally related compounds differ only in the number and placement of methyl groups on the polar head of the molecule and in the presence of double bonds in the side chain. Interestingly, although the typical American diet contains 2–4 times as much γ-TOH as α-TOH (1, 2), α-TOH is present in the serum and tissues at levels 5–6 times that of γ-TOH (3). This preferential accumulation of α-TOH in tissues, termed the α-TOH phenotype, is widely conserved in the animal kingdom and occurs despite the fact that all forms of vitamin E exhibit roughly similar radical scavenging activities (4, 5). Although in vitro and animal studies have suggested both beneficial (6–9) and detrimental (10) biological actions of non-α-TOH forms of vitamin E, the biological advantage of the α-TOH phenotype remains elusive.

The microsomal cytochrome P450 (CYP) enzymes catalyze a vast number of catalytic reactions, including the metabolism of lipids, steroids, and xenobiotics. These endoplasmic reticulum-bound enzymes require NADPH and the coenzyme cytochrome P450 reductase (CPR) for the source and transfer of electrons to the CYP enzyme. We previously identified cytochrome P450 4F2 (CYP4F2) as a human vitamin E-ω-hydroxylase (11), catalyzing the hydroxylation of one of the terminal methyl groups of the hydrophobic side chain. This ω-hydroxylation can be followed by oxidation to the corresponding carboxyl form and a series of side-chain shortening steps, ultimately leading to the formation of the 3′ and 5′ carboxychromanol metabolites that can be excreted in the urine (12–14). CYP4F2 displays substrate preference, such that

This work was supported by National Institutes of Health Grants DK-007158 and DK-067494. Its contents are solely the responsibility of the authors and do not necessarily represent the official views of the National Institutes of Health.

Manuscript received 24 July 2012 and in revised form 11 September 2012.

Published, JLR Papers in Press, September 11, 2012
DOI 10.1194/jlr.M030734

Abbreviations: CPR, cytochrome P450 reductase; CYP, cytochrome P450; CYP4F2, cytochrome P450 4F2; HIM, human intestinal microsome; HLM, human liver microsome; T3, tocotrienol; TOH, tocopherol.

[1]To whom correspondence should be addressed.
e-mail: rsp3@cornell.edu

non-α-TOH forms of vitamin E are metabolized to a greater extent than α-TOH, thereby contributing to the α-TOH phenotype (15).

Using a novel *Cyp4f14* knockout mouse model, we recently identified CYP4F14 as the major mouse vitamin E-ω-hydroxylase (ω-0, hydroxylation of a terminal methyl group), accounting for 70–90% of whole-body ω-hydroxy metabolite production (16). This result demonstrated the existence of other liver vitamin E-ω-hydroxylase enzyme(s) in the mouse. In addition, two novel metabolites were found to be excreted in the feces: 12′- and 11′-OH metabolites of δ- and γ-TOH, products of ω-1 and ω-2 hydroxylation activities, respectively. Interestingly, *Cyp4f14*$^{-/-}$ mice displayed increased fecal excretion of these novel metabolites as well as increased fecal excretion of unmetabolized TOH. Despite these counterbalancing mechanisms and redundancy in the TOH-ω-hydroxylase pathway, *Cyp4f14*-null mice fed a modest amount of γ-TOH in the form of soybean oil accumulated 2-fold more γ-TOH than wild-type mice. Although the urine has been previously considered to be the major route of TOH metabolite excretion, we found the fecal route to predominate over the urine.

The central hypothesis of the current work was that postabsorptive catabolism via TOH-hydroxylases constitutes the major limitation on tissue accumulation of non-α-TOH. We aimed to investigate whether dietary supplementation with high levels of γ- and δ-TOH would overcome the counterbalancing effects and result in tissue enrichment above that seen with the previous soybean oil diet. Two experimental models were employed: mice with global disruption of *Cyp4f14,* and mice with liver-specific CPR disruption that therefore lack all hepatic microsomal P450 activity. The L-*Cpr* model also allowed the opportunity to determine whether tissues other than the liver possess TOH-hydroxylase activity. Additionally, we extended the previous findings concerning novel ω-1 and ω-2 hydroxylase activities to determine their potential relevance in humans.

MATERIALS AND METHODS

Materials

Modified AIN-93G rodent diets were manufactured by DYETS (Bethlehem, PA). Tocopherols were obtained from Matreya, LLC (Pleasant Gap, PA). Bovine serum albumin, NADPH, β-glucuronidase (from *Escherichia coli*), and sulfatase (from *Aerobacter aerogenes*), protease inhibitor cocktail (catalog number P2714), PMSF, EDTA, and glycerol were purchased from Sigma-Aldrich (St. Louis, MO). Pooled human liver microsomes (HLM) and pooled human small intestine mucosal microsomes (HIM) were purchased from BD Biosciences (San Jose, CA). The internal standards d_9-α-TOH and d_9-α-CEHC were custom synthesized by J. Swanson (Cornell University, Ithaca, NY).

Tocopherol metabolism and tissue accumulation in *Cyp4f14*$^{-/-}$ mice supplemented with γ- and δ-TOH

Use of mice was in accordance with protocols approved by the Cornell Institutional Animal Care and Use Committee and following the National Institutes of Health guidelines for laboratory animal use. *Cyp4f14*$^{-/-}$ mice, which are viable and fertile, and their wild-type littermates, were generated as described previously (16). At 21 days of age, six mice of each genotype (three males and three females) were weaned onto a modified AIN-93G semipurified diet containing 12 mg/kg α-TOH and supplemented with 800 mg/kg each δ-TOH and γ-TOH. After 12 weeks, 24 h urine and fecal collections were made as described below. Mice were deeply anesthetized by isoflurane inhalation and exsanguinated via cardiac puncture. If bile was present in the gallbladder, it was collected with a syringe and frozen at −80°C until analysis. Heparinized blood was centrifuged at 6,000 *g* for 5 min, and serum was frozen at −80°C until analysis. Liver, kidney, lung, heart, abdominal fat, and brain tissue samples were flash frozen in liquid nitrogen for vitamin E quantification by gas chromatography-mass spectrometry (GC-MS) as described previously (16). Proximal small intestine samples were flash frozen for CYP4F14 expression analysis by RT-PCR.

Tocopherol metabolism and tissue accumulation in liver-specific *Cpr*$^{-/-}$ (L-*Cpr*$^{-/-}$) mice supplemented with γ- and δ-TOH

L-*Cpr*$^{-/-}$ mice, which have trace liver CYP activity by 2 months of age, and their wild-type littermates were generated as described previously (17). At 2.5 months of age, four male mice of each genotype were fed a modified AIN-93G semipurified diet containing 12 mg/kg α-TOH and supplemented with 800 mg/kg each δ-TOH and γ-TOH. After 4 weeks, 24 h urine and fecal collections were made as described below. Mice were then euthanized, and plasma and several tissues were collected as described above. Approximately 0.6 g of fresh liver was immediately used for preparation of microsomes as described below.

24 h urine and fecal collections

Mice were placed individually in wire bottom polycarbonate cages in which urine and fecal pellets were collected separately. Mice were afforded continuous access to food and water, and collections were made over 24 h following a 24 h acclimation period.

Preparation of liver microsome

Microsomes were prepared from fresh mouse liver by standard differential centrifugation as previously described, resuspended in 0.1 M sodium phosphate (NaP) buffer containing 1 mM EDTA and frozen at −80°C (16). Microsomal protein concentrations were determined by a Bradford-based Bio-Rad assay using BSA as the standard.

Preparation of intestinal mucosa microsome

Mice were euthanized by isoflurane exposure, and the upper 12 cm of the small intestine was immediately excised and placed on an ice-cold sheet of glass. The removed piece was immediately flushed with ice-cold wash buffer (0.9% NaCl containing 1 mM EDTA and 1 mM PMSF), then cut longitudinally, opened, and rinsed with ice-cold wash buffer to remove intestinal contents. The mucosal cells were gently scraped off with a razor blade. The intestinal mucosal cells were homogenized using a Teflon/glass homogenizer with ice-cold homogenization buffer [50 mM Tris-HCl, pH 7.4, containing 150 mM potassium chloride (KCl), 1 mM EDTA, 20% glycerol, 1 mM PMSF, and 10% protease inhibitor cocktail] and centrifuged at 10,000 *g* for 20 min at 4°C. The supernatant was centrifuged at 100,000 *g* for 1 h at 4°C. The microsomal pellet was resuspended in 0.1 M NaP buffer containing 1 mM EDTA and frozen at −80°C. Microsomal protein concentration was determined by a Bradford-based Bio-Rad assay.

Microsomal vitamin-E-ω-hydroxylase activity

Microsomes from L-*Cpr*$^{+/+}$ and L-*Cpr*$^{-/-}$ mouse liver and small intestine mucosa were assayed for ω-hydroxylase activity using γ-TOH, δ-TOH, and α-TOH as substrates complexed with BSA as described (15). The reaction system (0.5 ml) consisted of 0.1 M NaP buffer (pH = 7.4), 1.0 mM NADPH, and 100 μg microsomal protein. Substrate concentrations were 80 μmol/l for γ- and δ-TOH and 250 μmol/l for α-TOH to account for differences in microsomal uptake of each form of vitamin E (15). Following incubation at 37°C for 1 h, hydroxylation products were extracted, derivatized, and quantified by GC-MS as previously described (15), using d_9-α-TOH as internal standard. Activity was additionally evaluated in *Cyp4f14*$^{+/+}$ and *Cyp4f14*$^{-/-}$ small intestinal microsomes using γ-TOH as substrate.

Analysis of TOH and metabolites in 24 h urine and fecal samples

Twenty-four hour fecal collections were homogenized in PBS, and an aliquot was used for analysis. Urine and fecal samples were incubated with β-glucuronidase (800 units for urine or 1,600 units for feces, dissolved in NaP buffer, pH 6.8) and sulfatase (0.4 units for urine or 0.8 units for feces) for 2 h at 37°C. Samples were acidified to pH 2, extracted, and derivatized as previously described (16). TOH and their metabolites were quantified by GC-MS using d_9-α-TOH and d_9-α-CEHC as internal standards.

Analysis of bile TOH and metabolites in *Cyp4f14*$^{+/+}$ and *Cyp4f14*$^{-/-}$ mice

Bile samples from *Cyp4f14* mice (two wild-type and three knockout) were incubated with enzymes (800 units β-glucuronidase, 0.4 units sulfatase) for 2 h at 37°C. Samples were then acidified and extracted as described above for urine.

Suitability of methods for detection of TOH metabolites in human fecal material

In an exploratory investigation, reference fecal material was obtained from an adult male following 14 days supplementation of either γ-TOH or α-TOH (400 mg/kg/day). Samples were processed and analyzed for TOH metabolites as described above for mice.

Vitamin E-ω-hydroxylase activity of human liver and intestinal microsomes

Pooled human liver microsomes (HLM) and pooled human intestinal mucosa microsomes (HIM) were assayed for vitamin E-ω-hydroxylase activity using γ-TOH (80 μM), δ-TOH (80 μM), and α-TOH (250 μM) as substrates. The reaction system (0.5 ml) consisted of 0.1 M NaP buffer containing 0.1 mM EDTA (pH 7.4), 2.0 mM NADPH, and 200 μg microsomal protein. Following incubation at 37°C for 1 h, reaction products were extracted, derivatized, and quantified by GC-MS as described above.

Statistical analysis

All tocopherols and tocopherol metabolites were log transformed as necessary, and means were compared between wild-type and knockout mice using Student *t*-test. Additionally, tissue TOH concentrations in *Cyp4f14*$^{-/-}$ mice were compared using a two-way ANOVA with genotype and gender as main effects, as well as the interaction effect. When the interaction effect was not significant, it was removed from the model. All tests were two-sided, and a *P*-value < 0.05 was considered statistically significant. Analyses were performed using JMP version 8 (SAS Institute).

RESULTS

Effect of *Cyp4f14* disruption on 24 h TOH and TOH metabolite excretion

Metabolic cages were utilized to obtain 24 h urine and fecal samples from *Cyp4f14*$^{+/+}$ and *Cyp4f14*$^{-/-}$ mice fed 800 mg/kg of both δ- and γ-TOH for 12 weeks. In urine, only 3′- and 5′-carboxychromanol metabolites of δ- and γ-TOH were detected. Urinary metabolites of γ-TOH were reduced by 88% and those of δ-TOH were reduced by 77% in *Cyp4f14*$^{-/-}$ mice compared with their wild-type littermates. Total urinary tocopherol metabolites were reduced by 82% in *Cyp4f14*$^{-/-}$ mice (**Table 1**).

Analysis of 24 h fecal samples revealed the presence of all six carboxychromanol metabolites, as well as the 13′-OH metabolites of γ- and δ-TOH, formed via the ω-oxidation pathway (**Table 2**). The 13′-COOH metabolite was consistently the predominant ω-oxidation metabolite in fecal samples. Total ω-oxidation metabolites of γ-TOH were reduced by 79% and those of δ-TOH by 89% in *Cyp4f14*$^{-/-}$ mice. 12′-OH and 11′-OH metabolites of γ- and δ-TOH were also present, formed via the ω-1 and ω-2 oxidation pathways, respectively. These metabolites were also detected in the limited number of gallbladder bile samples that were collected (data not shown).

Twenty-four hour whole-body (urine + fecal) ω-oxidation metabolites of γ- and δ-TOH were reduced by 82% in *Cyp4f14*$^{-/-}$ compared with wild-type mice (**Fig. 1A**). The sum of 24 h ω-1 and ω-2 metabolites of γ- and δ-TOH, although numerically higher in *Cyp4f14*$^{-/-}$ mice (30%), was not statistically significantly altered by the disruption of *Cyp4f14*. As a result, the combination of metabolites from all three pathways was 40% reduced in *Cyp4f14*$^{-/-}$ mice. Twenty-four hour fecal excretion of unmetabolized TOH was not statistically different between wild-type and *Cyp4f14*-null mice (Fig. 1B).

TABLE 1. 24 h urinary metabolite excretion in *Cyp4f14*$^{+/+}$ and *Cyp4f14*$^{-/-}$ mice supplemented with γ- and δ-TOH

	Urinary Metabolites[a]				
	γ-3′-COOH	γ-5′-COOH	δ-3′-COOH	δ-5′-COOH	Total
Cyp4f14$^{+/+}$	185.9 ± 114.0	133.3 ± 47.9	232.2 ± 111.7	162.1 ± 54.8	713.6 ± 243.6
Cyp4f14$^{-/-}$	29.3 ± 14.0	9.6 ± 4.8[b]	60.1 ± 11.7	29.6 ± 15.1	128.6 ± 42.2[b]
% Reduction	84%	93%	74%	82%	82%

Mice were fed the supplemented diet for 12 weeks after weaning. Values represent mean ± SEM (n = 4).
[a]nmol/24 h.
[b]Significantly different from Cyp4f14$^{+/+}$ mice ($P < 0.05$). The 3′- and 5′-COOH metabolites of α-TOH were not detected.

TABLE 2. 24 h fecal metabolite excretion in *Cyp4f14*$^{+/+}$ and *Cyp4f14*$^{-/-}$ mice supplemented with γ- and δ-TOH

	Cyp4f14 Genotype	ω-0 Oxidation Products[a]							ω-1, 2 Metabolites[a]		
		3′-COOH	5′-COOH	7′-COOH	9′-COOH	11′-COOH	13-COOH	13′-OH	ω-0 Total[a]	11′-OH	12′-OH	Total[a]
γ-TOH	+/+	4.14 ± 1.81	10.8 ± 3.41	0.29 ± 0.04	11.3 ± 2.17	18.7 ± 4.53	53.6 ± 14.2	28.9 ± 5.20	127.7 ± 51.4	30.9 ± 2.15	222.0 ± 16.9	380.5 ± 29.1
	−/−	0.55 ± 0.32	1.21 ± 0.37[b]	0.07 ± 0.02	1.3 ± 0.66[b]	15.3 ± 4.99	3.1 ± 1.2[b]	5.7 ± 1.44[b]	27.2 ± 16.1[b]	54.6 ± 9.18	347.0 ± 55.8	428.8 ± 70.3
δ-TOH	+/+	5.39 ± 2.79	14.1 ± 4.34	0.35 ± 0.05	4.64 ± 0.44	4.98 ± 0.67	93.1 ± 19.5	12.0 ± 2.22	134.6 ± 52.0	37.1 ± 3.44	157.6 ± 18.3	329.4 ± 21.9
	−/−	0.92 ± 0.50	1.9 ± 0.45[b]	0.11 ± 0.02[b]	0.71 ± 0.16[b]	2.83 ± 0.48[b]	3.95 ± 0.89[b]	3.9 ± 0.95[b]	14.4 ± 4.7[b]	50.2 ± 10.9	201.5 ± 37.9	266.1 ± 49.4

Mice were fed the supplemented diet for 12 weeks after weaning. Values represent mean ± SEM (n = 4).
[a] nmol/24 h.
[b] Significantly different from Cyp4f14$^{+/+}$ mice ($P < 0.05$). Metabolites of α-TOH were undetectable or at trace levels.

Tissue TOH status of *Cyp4f14*$^{+/+}$ and *Cyp4f14*$^{-/-}$ supplemented with γ- and δ-TOH

Cyp4f14$^{-/-}$ mice displayed significantly higher tissue concentrations of δ-TOH in the plasma, lung, and liver, averaging a 70% increase in these tissues compared with wild-type mice. *Cyp4f14*$^{-/-}$ mice also had significantly higher γ-TOH in the plasma, lung, kidney, liver, and brain, averaging a 90% increase in these tissues compared with wild-type mice (Fig. 1C). The tissues with the largest difference from wild-type mice were plasma for δ-TOH (2.2-fold higher than wild-type) and brain for γ-TOH (2.7-fold higher than wild-type). A gender effect was observed for many forms of vitamin E, such that females had significantly higher levels of TOH in several tissues. These gender differences were observed in the plasma (γ-, δ-TOH), lung (α-, γ-, δ-TOH), kidney (γ-, δ-TOH), liver (α-, γ-, δ-TOH), heart (α-TOH), brain (α-, γ-, δ-TOH), and fat (δ-TOH) (data not shown). Except for δ-TOH in the plasma, the interaction effect was not significant, indicating that the effect of *Cyp4f14* disruption on tissue TOH concentration did not differ by gender.

Effect of liver-specific *Cpr* disruption on liver microsomal TOH-ω-hydroxylase activity and TOH metabolism and excretion

Wild-type mice displayed robust hepatic microsomal ω-hydroxylase activity toward γ-TOH (101 pmol product/min/mg protein) and δ-TOH (125 pmol product/min/mg protein). In contrast, L-*Cpr*$^{-/-}$ mice exhibited no detectable ω-hydroxylase activity toward either substrate in liver microsomal activity assays, indicating the complete loss of liver TOH-ω-hydroxylase activity. Urinary metabolites (3′- and 5′-carboxychromanols) of γ-TOH were reduced by 56% and those of δ-TOH were reduced by 72% in L-*Cpr*$^{-/-}$ mice compared with their wild-type littermates. Total urinary tocopherol metabolites (sum of γ- and δ-TOH metabolites) were reduced by 70% in L-*Cpr*$^{-/-}$ mice (**Table 3**). Mice of both genotypes excreted substantially more metabolites of δ-TOH than γ-TOH, despite similar concentrations of the two TOH in the diet. Analysis of 24 h fecal samples revealed the presence of all previously identified ω-0, ω-1, and ω-2 metabolites of γ- and δ-TOH, except 7′-COOH-γ-TOH (**Table 4**). As was the case with *Cyp4f14* mice, the 13′-COOH was the predominant ω-oxidation metabolite in fecal samples. Twenty-four hour whole-body (urine + fecal) ω-oxidation metabolites of γ- and δ-TOH were reduced by 70% in L-*Cpr*$^{-/-}$ mice compared with wild-type mice, whereas ω-1 and ω-2 metabolites were unchanged (**Fig. 2A**). The sum of metabolites of both TOH from all three pathways was 66% lower in L-*Cpr*$^{-/-}$ mice. Fecal excretion of unmetabolized TOH was greater in L-*Cpr*$^{-/-}$ mice compared with wild-type mice for α-TOH (2.4-fold), γ-TOH (3.2-fold), and δ-TOH (6.6-fold; Fig. 2B).

Tissue TOH status of L-*Cpr*$^{+/+}$ and L-*Cpr*$^{-/-}$ mice supplemented with γ- and δ-TOH

α-TOH concentrations in L-*Cpr*$^{-/-}$ mice were half those of wild-type mice in every tissue analyzed (Fig. 2C). δ-TOH concentrations in the lung, heart, and fat of L-*Cpr*$^{-/-}$ mice were, on average, 43% those of wild-type mice. No other significant differences in tissue TOH status between genotypes were observed.

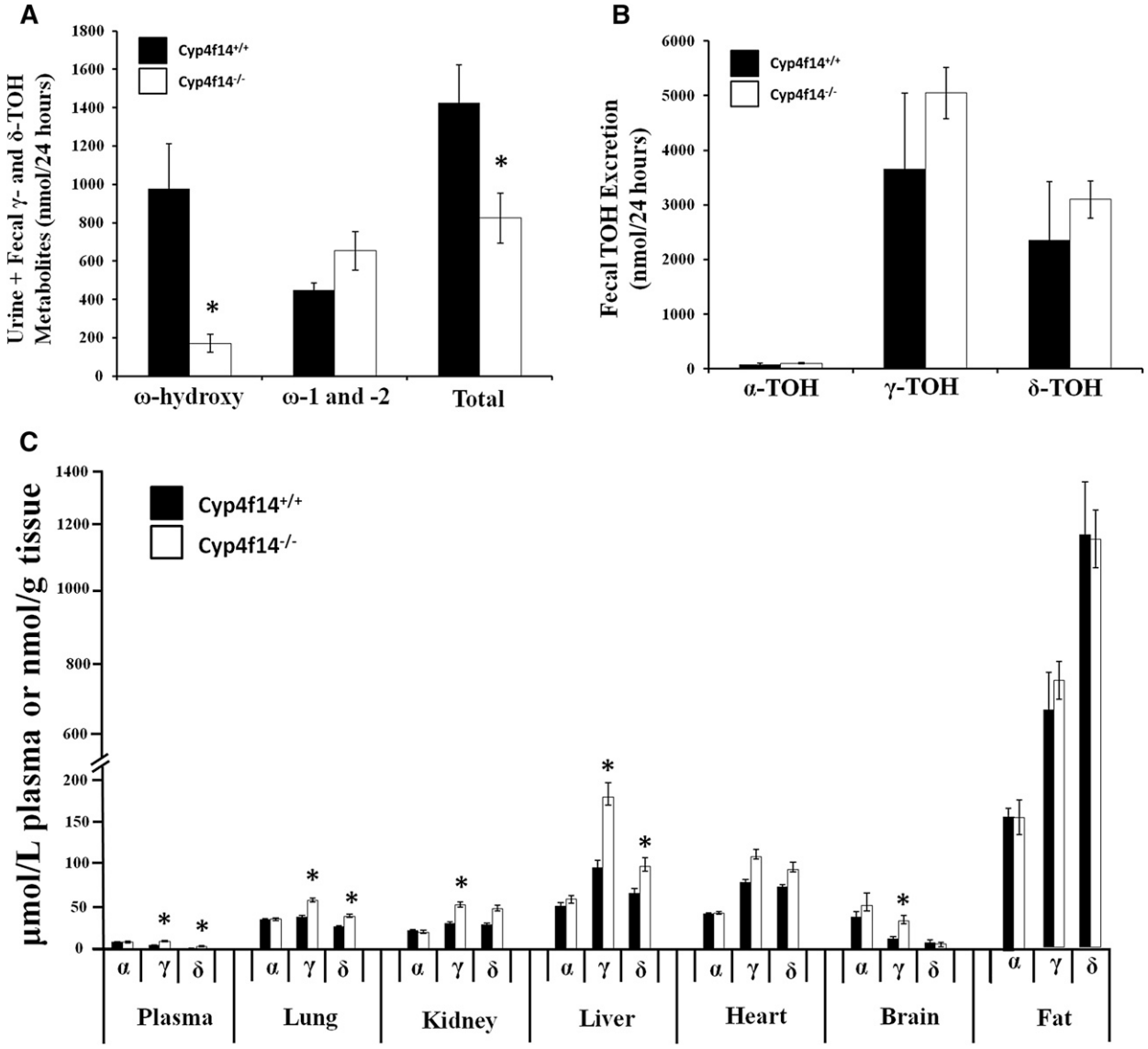

Fig. 1. Effect of *Cyp4f14* disruption on vitamin E metabolism and tissue accumulation in mice supplemented with γ- and δ-TOH for 12 weeks. A: 24 h ω-hydroxy, ω-1/ω-2 hydroxy and total vitamin E metabolite excretion in wild-type (solid bar) and *Cyp4f14*$^{-/-}$ mice (open bar) were quantified by GC-MS. Asterisks indicate significant differences from wild-type. B: 24 h fecal excretion of unmetabolized TOH in wild-type (solid bar) and *Cyp4f14*$^{-/-}$ mice (open bar). C: Concentration of TOH in plasma and tissues of wild-type (solid bar) and *Cyp4f14*$^{-/-}$ mice (open bar) fed the supplemented diet for 12 weeks. Asterisks indicate significant differences from wild-type mice ($P < 0.05$).

Intestinal microsomal vitamin E-ω-hydroxylase activity in L-*Cpr*$^{+/+}$, L-*Cpr*$^{-/-}$, *Cyp4f14*$^{+/+}$, and *Cyp4f14*$^{-/-}$ mice

Microsomes prepared from small intestinal mucosa of L-*Cpr*$^{+/+}$ and L-*Cpr*$^{-/-}$ mice displayed vitamin E-ω-hydroxylase activity toward α-, γ-, and δ-TOH. In the absence of product sufficient for definitive mass spectral identification using GC-MS in scan mode, the intestinal 13′-OH oxidation products were tentatively identified on the basis of retention times (13.6, 10.2, and 8.4 min, respectively), expected molecular ions (590.6, 576.6, and 562.6, respectively), expected fragment ions (237.0, 223.0, and 209.0, respectively) and their ratios (**Fig. 3D–F**), as compared

TABLE 3. 24 h urinary metabolite excretion in L-*Cpr*$^{+/+}$ and L-*Cpr*$^{-/-}$ mice supplemented with γ- and δ-TOH

	Urinary Metabolites[a]				
	γ-3′-COOH	γ-5′-COOH	δ-3′-COOH	δ-5′-COOH	Total
L-*Cpr*$^{+/+}$	43.8 ± 4.49	37.5 ± 3.11	633.3 ± 34.4	56.4 ± 8.74	771.0 ± 43.9
L-*Cpr*$^{-/-}$	21.5 ± 3.83[b]	14.0 ± 3.36[b]	166.5 ± 28.5[b]	28.3 ± 7.86	230.3 ± 41.3[b]
% Reduction	51%	63%	74%	50%	70%

Mice were fed the supplemented diet for 4 weeks. Values represent mean ± SEM (n = 4).
[a] nmol/24 h.
[b] Significantly different from L-*Cpr*$^{+/+}$ mice ($P < 0.05$). The 3′- and 5′-COOH metabolites of α-TOH were not detected.

TABLE 4. 24 h fecal metabolite excretion in L-$Cpr^{+/+}$ and L-$Cpr^{-/-}$ mice supplemented with γ- and δ-TOH

		ω-0 Oxidation Products[a]							ω-1, 2 Metabolites[a]		
	L-*Cpr* Genotype	3′-COOH	5′-COOH	7′-COOH	9′-COOH	11′-COOH	13-COOH	13′-OH	ω-0 Total[a]	11′-OH	12′-OH	Total[a]
γ-TOH	+/+	15.5 ± 8.11	10.9 ± 1.98	ND	4.92 ± 0.96	9.23 ±2.08	71.1 ±22.7	19.6 ± 5.38	131.3 ± 59.7	3.09 ± 0.62	33.5 ± 6.51	167.8 ± 35.7
	−/−	0.79 ± 0.15[b]	1.74 ± 0.17[b]	ND	2.84 ± 0.58	7.32 ±0.58	20.8 ± 2.11[b]	7.13 ± 1.15	40.6 ±5.4[b]	2.62 ± 0.26	23.5 ± 0.80	66.7 ± 3.61[b]
δ-TOH	+/+	43.8 ± 19.9	39.1 ± 6.74	0.53 ± 0.12	3.73 ± 0.72	4.22 ±0.99	230.3 ± 61.5	30.8 ± 6.86	325.5 ± 172.3	12.7 ± 2.17	65.3 ± 16.1	430.3 ± 104.1
	−/−	3.01 ± 1.28 [b]	4.82 ± 1.06[b]	0.23 ± 0.08	2.37 ± 0.56	1.74 ± 0.24[b]	63.6 ± 3.71[b]	13.5 ± 1.90[b]	89.2 ±9.7[b]	8.67 ± 0.55	65.6 ± 8.46	163.5 ± 4.74[b]

Mice were fed the supplemented diet for 4 weeks. Values represent mean ± SEM (n = 4).
[a] nmol/24 h.
[b] Significantly different from L-$Cpr^{+/+}$ mice ($P < 0.05$). Metabolites of α-TOH were not detected (ND) or at trace levels.

with the metabolites formed by liver microsomes from L-$Cpr^{+/+}$ mice (Fig. 3A–C) using GC-MS in SIM mode. The rank order of activity (rate of metabolite production) by substrate for mouse intestinal microsomes was γ>δ>>α and that for mouse liver was γ=δ>>α. Mouse intestinal microsomes displayed ω-hydroxylase activity that was 10% that of mouse liver microsomes for the three substrates. Intestinal microsomes from *Cyp4f14*$^{+/+}$ and *Cyp4f14*$^{-/-}$ mice were also compared for activities toward γ-TOH. Microsomes from *Cyp4f14*$^{+/+}$ displayed γ-TOH-ω-hydroxylase activity, whereas those from *Cyp4f14*$^{-/-}$ mice had no detectable activity (data not shown). RT-PCR analysis of proximal small intestine samples confirmed the absence of *Cyp4f14* mRNA in *Cyp4f14*$^{-/-}$ mice (data not shown).

TOH-ω-hydroxylase activity in human intestine microsomes and human liver microsomes

HLM and HIM displayed ω-hydroxylase activity toward δ-, γ-, or α-TOH (**Fig. 4**). The rank order of activity (rate of metabolite production) by substrate for HLM was γ>δ>>α and that for HIM was γ=δ>>α. HIM displayed ω-hydroxylase activity that was 20–30% that of HLM for the three substrates.

TOH metabolites in human fecal material

Fecal material from an individual supplemented with 400 mg/kg/day γ-TOH contained all six γ-carboxychromanol metabolites, as well as the 13′-OH, 12′-OH, and 11′-OH metabolites. The sum of ω-0 oxidation metabolites represented 80% of total fecal metabolites with the remaining 20% composed of the 12′-OH and 11-OH metabolites. Fecal material from the same individual supplemented with 400 mg/kg/day α-TOH contained the 3′, 7′, and 11′-α-carboxychromanols and the 13′-OH, 12′-OH, and 11′-OH metabolites of α-TOH. ω-0 Oxidation metabolites represented 30% of total metabolites, whereas the 12′-OH (ω-1) and 11′-OH (ω-2) metabolites composed the remaining 70%.

DISCUSSION

We previously reported that CYP4F14 is the major vitamin E-ω-hydroxylase in the mouse and that its disruption in mice fed a soybean oil diet containing modest amounts of γ-TOH resulted in elevated tissue levels of γ-TOH relative to wild-type mice (16). The accumulation of γ-TOH occurred despite two counterbalancing mechanisms, namely, *i*) higher excretion of unmetabolized γ-TOH and *ii*) elevated excretion of novel ω-1 and ω-2 metabolites of γ-TOH. The previous studies also revealed the presence in mice of ω-hydroxylase activity not mediated by CYP4F14. The current work aimed to further characterize the role of vitamin E-ω-hydroxylase in limiting tissue accumulation of TOH. Specifically, we investigated whether dietary supplementation with high levels of γ- and δ-TOH would overcome the counterbalancing effects and result in tissue enrichment above that seen with the previous soybean oil diet. Two experimental models were employed: mice with global disruption of *Cyp4f14* and mice with liver-specific

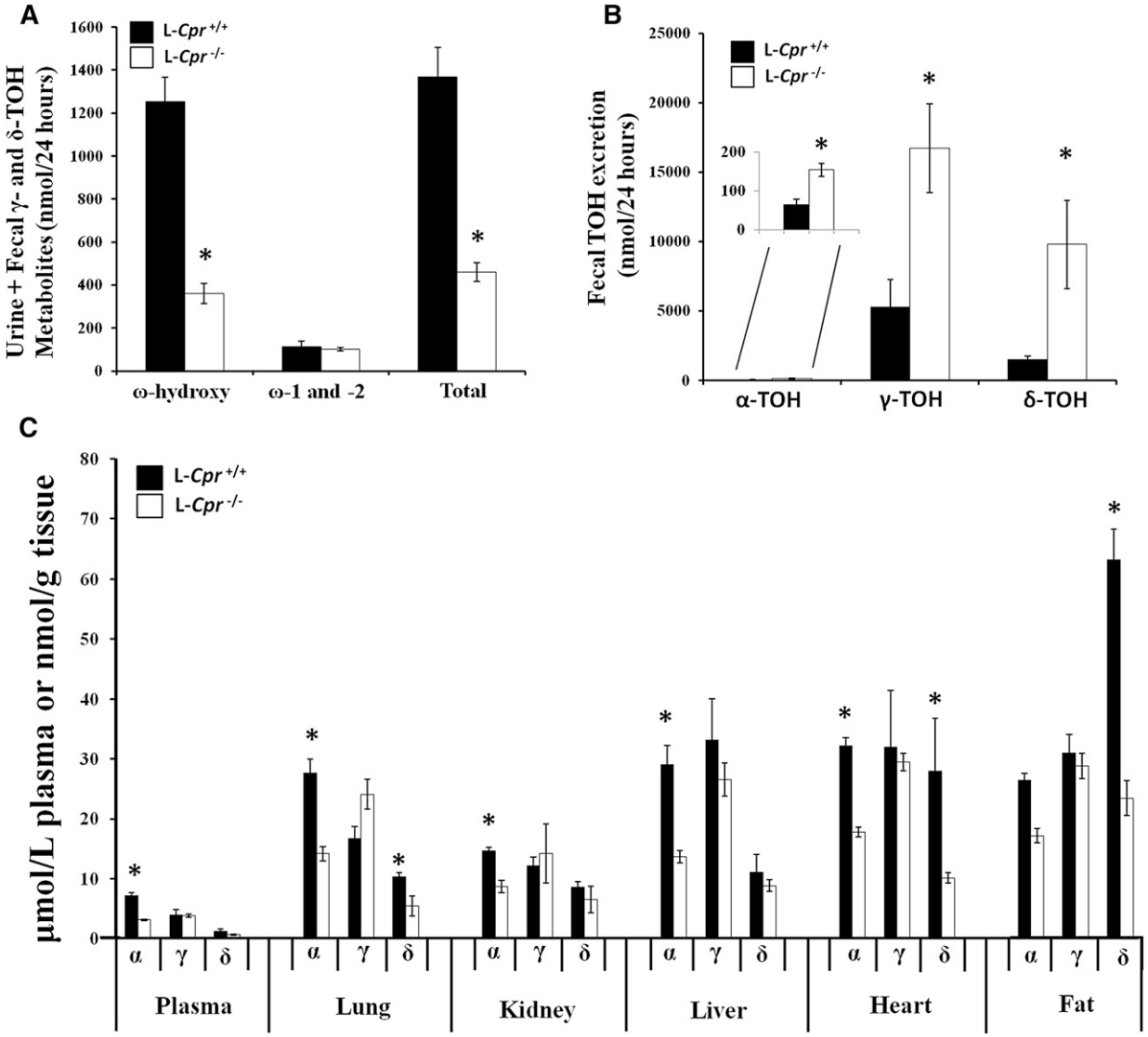

Fig. 2. Effect of the L-*Cpr* disruption on vitamin E metabolism and tissue accumulation in mice supplemented with γ- and δ-TOH for 4 weeks A: 24 h ω-hydroxy, ω-1/ω-2 hydroxy and total vitamin E metabolite excretion in wild-type (solid bar) and L-$Cpr^{-/-}$ mice (open bar) were quantified by GC-MS. Asterisks indicate significant differences from wild-type. B: 24 h fecal excretion of unmetabolized TOH in wild-type (solid bar) and L-$Cpr^{-/-}$ mice (open bar). C: Concentration of TOH in plasma and tissues of wild-type (solid bar) and L-$Cpr^{-/-}$ mice (open bar) fed the supplemented diet for 4 weeks. Asterisks indicate significant differences from L-$Cpr^{-/-}$ mice ($P < 0.05$).

disruption of *Cpr*, both supplemented with high levels of γ- and δ-TOH.

Supplementation with γ- and δ-TOH resulted in substantial increases in tissue levels of these forms in both wild-type and *Cyp4f14* knockout mice in comparison to mice previously fed an unsupplemented soybean oil diet (16). The increases in tissue levels (7- to 25-fold) were similar or greater than the increase in dietary levels (5- to 10-fold). Although the fold-difference in tissue γ- and δ-TOH between knockout and wild-type mice was similar to that previously observed in unsupplemented mice, the absolute difference in tissue levels was substantially greater. For example, the effect of *Cyp4f14* disruption resulted in an increase of 14 nmol/g γ-TOH in the liver of unsupplemented mice (16) but an increase of 100 nmol/g in liver of supplemented mice (Fig. 1C), despite being a 2-fold difference between genotypes in both cases. The dramatic elevation in tissue γ- and δ-TOH occurred in the absence of any overt detrimental effects. The combination of supplementation and *Cyp4f14* disruption resulted in a 14-fold increase (186 nmol/g) in liver γ-TOH (Fig. 1C), illustrating the potential of this model to study the biological consequences of tissue enrichment with specific forms of vitamin E.

Interestingly, female mice accumulated significantly more vitamin E in many tissues compared with their male counterparts, irrespective of genotype. Due to the small sample size when segregated by gender, statistical analysis of metabolic cage data was not possible, although it appears that females neither metabolize vitamin E nor excrete unmetabolized TOH to a lesser extent than males. The reason for this gender effect and its consequences are unknown but warrants further investigation.

Unlike any other tissue in *Cyp4f14*$^{-/-}$ and wild-type mice, adipose tissue displayed higher levels of δ-TOH compared

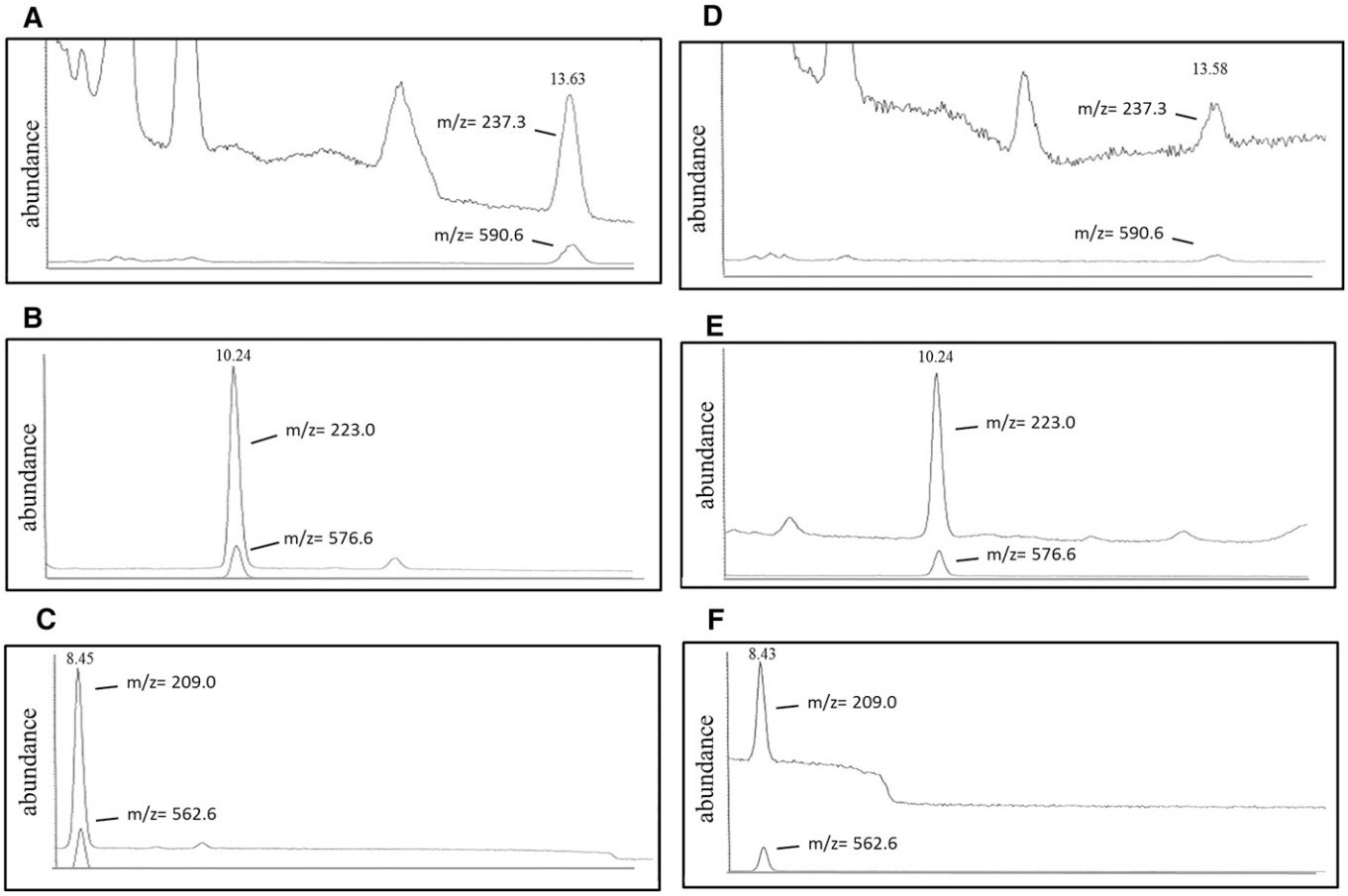

Fig. 3. Evidence of TOH-ω-hydroxylase activity in microsomes prepared from mouse liver (A–C) and small intestinal mucosa (D–F). GC-MS chromatograms from incubations of liver microsomes from L-*Cpr*$^{+/+}$ mice with (A) 250 μM α-TOH, (B) 80 μM γ-TOH, and (C) 80 μM δ-TOH, illustrating formation of the corresponding 13′-OH metabolites. Microsomes from L-*Cpr*$^{-/-}$ mouse small intestinal mucosa were incubated with (D) 250 μM α-TOH, (E) 80 μM γ-TOH, and (F) 80 μM δ-TOH, illustrating formation of the corresponding 13′-OH metabolites and demonstrating vitamin E-ω-hydroxylase activity in mouse intestine. Retention times and the ratio of the molecular ion to the fragment ion of intestinal samples were consistent with that of the liver.

with γ-TOH, despite similar levels of these forms in the diet. One possible explanation for this finding is that adipose tissue may have vitamin E-metabolizing capability such that γ-TOH is being metabolized to a greater extent than δ-TOH. The concentration of δ-TOH was not affected by the disruption of *Cyp4f14*, indicating that any vitamin E-metabolizing capability in the adipose tissue is through a CYP4F14-independent mechanism. We observed higher levels of unmetabolized fecal γ-TOH than δ-TOH in both *Cyp4f14*$^{-/-}$ and wild-type mice, which could also be contributing to higher δ-TOH levels in adipose tissue.

Cyp4f14 disruption in supplemented mice resulted in substantial loss of whole-body vitamin E-ω-hydroxylase activity (80%), the magnitude of which was similar to that previously observed in unsupplemented mice (16). Although not statistically significant, the higher level of 11′- and 12′-OH metabolites excreted in the supplemented *Cyp4f14*$^{-/-}$ mice of the current study resulted in attenuation of the overall metabolic deficit, reducing the whole-body decrement in vitamin E metabolic activity to 40%. The counterbalancing effect of these alternative pathways remained an important mechanism in limiting tissue TOH accumulation in the context of supplementation.

Supplemented mice of both genotypes excreted substantial quantities of unmetabolized TOH in the feces, which constituted a significant mechanism of resistance to tissue TOH accumulation. Whether this resulted from decreased intestinal absorption or increased biliary secretion of tocopherols is unknown. In the supplemented mice, fecal TOH elimination was a more important means of disposal of dietary TOH than was metabolic elimination. In wild-type mice, fecal TOH elimination was five times that of whole-body metabolic disposal, whereas in knockout mice, fecal TOH disposal was 10-fold that of metabolic disposal. In this respect, fecal elimination of unmetabolized TOH served as a high-capacity mechanism of resisting tissue accumulation of dietary TOH under conditions of supplementation. These findings suggest that supplementation was not able to completely overcome the mechanisms of resistance of tissue accumulation constituted by vitamin E metabolism and fecal TOH excretion.

Mice exhibit multiple hepatic TOH-hydroxylase activities in the absence of CYP4F14 that influence diet-induced tissue levels of TOH. Therefore, we utilized L-*Cpr*$^{-/-}$ mice, in which all hepatic microsomal CYP activity was absent. If vitamin E-metabolizing capacity was restricted to the liver,

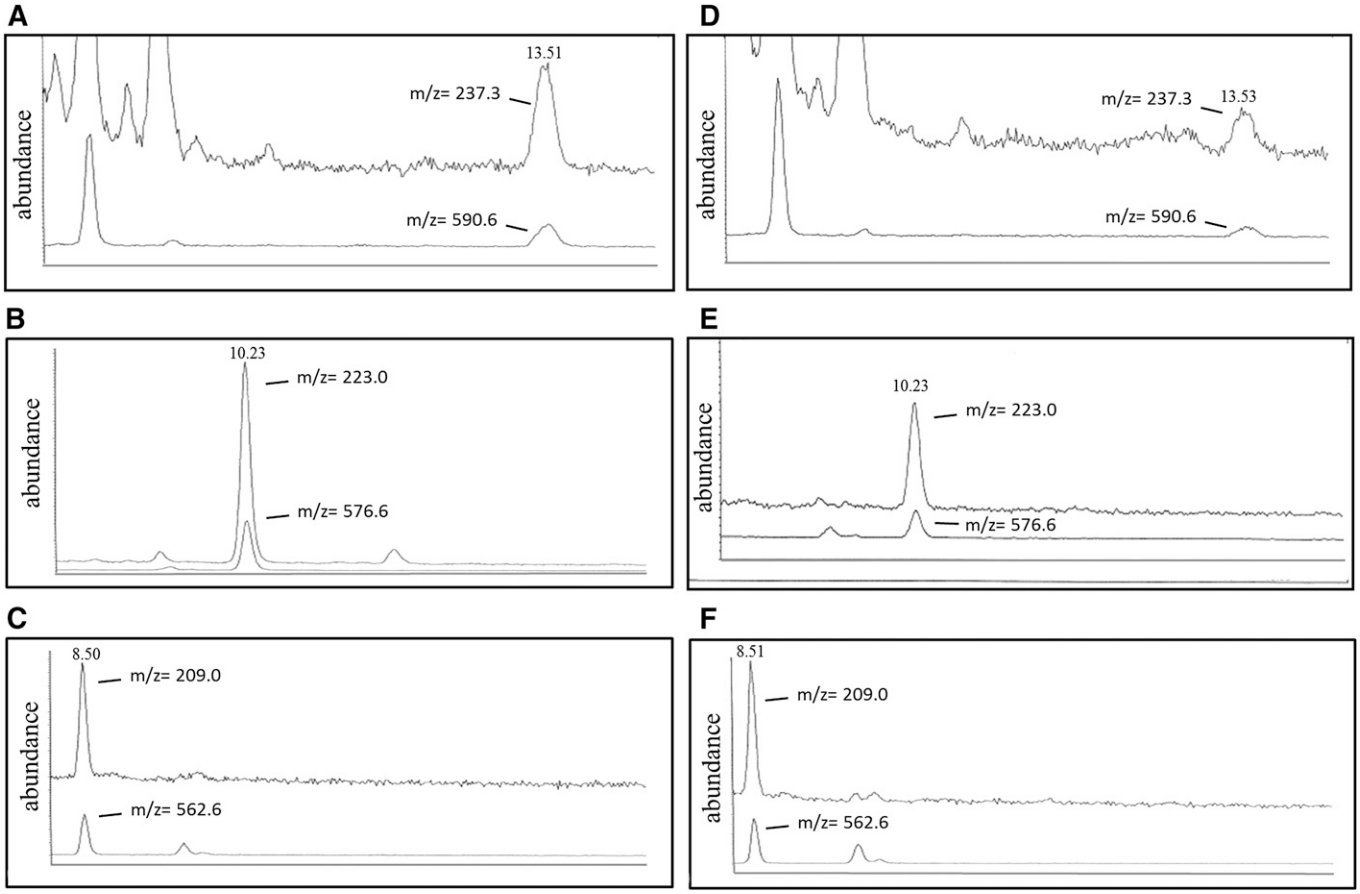

Fig. 4. TOH-ω-hydroxylase activity in pooled human liver microsomes (A–C) and pooled human intestinal microsomes (D–F). GC-MS chromatograms from incubations of human liver microsomes with (A) 250 μM α-TOH, (B) 80 μM γ-TOH, and (C) 80 μM δ-TOH, illustrating formation of the corresponding 13′-OH metabolites. Human intestinal mucosal microsomes were incubated with (D) 250 μM α-TOH, (E) 80 μM γ-TOH, and (F) 80 μM δ-TOH, illustrating formation of the corresponding 13′-OH metabolites and demonstrating vitamin-E-ω-hydroxylase activity in human intestine. Retention times and the ratio of the molecular ion to the fragment ion of intestinal samples were consistent with that of the liver.

then these mice should completely lack the ability to metabolize vitamin E. However, in L-*Cpr*$^{-/-}$ mice supplemented with γ- and δ-TOH, whole-body metabolic capacity was only reduced by 70%, clearly demonstrating the presence of extra-hepatic ω, ω-1, and ω-2 hydroxylation activities. This is the first report to show the existence of extra-hepatic vitamin E metabolic activity.

Despite significant reductions in vitamin E metabolism in L-*Cpr*$^{-/-}$ mice supplemented with γ- and δ-TOH, tissue levels of all three TOH were similar to or actually lower than those of wild-type mice. This finding may have resulted from a reduced efficiency of TOH absorption secondary to the inability to synthesize bile acids. Liver-specific disruption of *Cpr* has been shown to cause 90% reduced bile acid production due to the disruption of CYP7A1 in the liver, the rate-limiting step of neutral bile acid biosynthetic pathway (18). This feature additionally complicates the interpretation of the 70% reduction in whole-body in vivo metabolic capacity and could underestimate the magnitude of extra-hepatic metabolic activity.

Shin et al. reported *Cyp4f14* expression in the small intestine (19); therefore, we evaluated that tissue and found ω-hydroxylase activity toward several forms of vitamin E at levels approximately 10% that of the liver. TOH-ω-hydroxylase activity present in the intestine was shown to be mediated entirely by CYP4F14, as *Cyp4f14*$^{-/-}$ mice showed a complete absence of this activity. We conclude that mouse intestine, unlike the liver, has only one enzyme capable of TOH-ω-hydroxylase activity. We confirmed the presence of vitamin E hydroxylase activity in human small intestinal mucosa, validating the mouse as a model to investigate the role of the intestine in first-pass vitamin E metabolism. The contribution of the intestine to whole-body vitamin E metabolic activity is at present unknown but could be investigated given the availability of intestine-specific *Cpr* knockout mice (20).

The ω-1 and ω-2 hydroxylations of δ- and γ-TOH represented quantitatively important mechanisms of vitamin E metabolism, accounting for up to 30% of whole-body vitamin E metabolites in wild-type mice. The relevance of this finding to human vitamin E metabolism was demonstrated by the identification of all ω-0, ω-1, and ω-2 hydroxy metabolites of γ-TOH in human feces. We additionally identified several fecal ω-hydroxy metabolites and both ω-1 and

ω-2 metabolites of α-TOH, the most commonly used form of vitamin E supplement. The enzyme(s) responsible for the ω-1 and ω-2 oxidation of vitamin E in mice and humans are unknown. The finding of these metabolites in fecal material raised the possibility that they may have arisen from the action of gut microflora. However, this is unlikely as we observed no difference in their concentration in intestinal contents above versus below the cecum (data not shown). Additionally, ceacal samples, with or without a heat treatment sufficient to kill bacteria, were incubated for 24 h at 37°C, followed by treatment with deconjugation enzymes. The concentration of ω-1 and ω-2 metabolites was not affected by heat treatment, further supporting the lack of a role of intestinal microflora in the production of these novel metabolites. Zhao et al. reported the occurrence of several ω-0 oxidation products in mouse and human fecal material that likewise apparently did not arise by the action of intestinal microflora (21). The presence of these metabolites in the bile of mice indicates that these are likely of hepatic origin.

In summary, dietary supplementation with high levels of γ- and δ-TOH results in tissue enrichment of these forms of vitamin E in mice, and the enrichment was enhanced by the disruption of CYP4F14, the major murine TOH-ω-hydroxylase. However, at these high dietary levels of TOH, other mechanisms that serve to limit tissue enrichment were quantitatively more important than the ω-hydroxlyase pathway. These mechanisms consisted of the ω-1 and ω-2 hydroxylase pathways and fecal elimination of unmetabolized TOH, with the latter predominating under conditions of supplementation. The use of L-*Cpr*$^{-/-}$ mice, which completely lack liver microsomal P450 activity, including vitamin E-hydroxylase activity, revealed the presence of extrahepatic vitamin E metabolism in vivo. TOH-ω-hydroxylase activity was observed in the mucosa of the small intestine and was mediated entirely by CYP4F14. This represents the first report of a tissue other than the liver capable of metabolizing vitamin E. These findings were extended to humans with the observations of vitamin E-ω-hydroxylase activity in human intestinal mucosa and fecal excretion of ω-1 and ω-2 metabolites of γ- and α-TOH. The results of these investigations shed new light on the role of TOH-ω-hydroxlyase activity and other mechanisms in preventing diet-induced accumulation of vitamin E in mice, and they further characterize vitamin E metabolism in mice and humans.

REFERENCES

1. Bieri, J. G., and R. P. Evarts. 1973. Tocopherols and fatty acids in American diets. The recommended allowance for vitamin E. *J. Am. Diet. Assoc.* **62:** 147–151.
2. Dial, S., and R. R. Eitenmiller. 1995. Tocopherols and tocotrienols in key foods in the U.S. diet. *In* Nutrition, Lipids, Health, and Disease. A. S. H. Ong, E. Niki, and L. Packer, editors. AOCS Press, Champaign, IL. 327–342.
3. Ford, E. S., R. L. Schleicher, A. H. Mokdad, U. A. Ajani, and S. M. Liu. 2006. Distribution of serum concentrations of alpha-tocopherol and gamma-tocopherol in the US population. *Am. J. Clin. Nutr.* **84:** 375–383.
4. Yoshida, Y., E. Niki, and N. Noguchi. 2003. Comparative study on the action of tocopherols and tocotrienols as antioxidant: chemical and physical effects. *Chem. Phys. Lipids.* **123:** 63–75.
5. Saito, Y., Y. Yoshida, T. Akazawa, K. Takahashi, and E. Niki. 2003. Cell death caused by selenium deficiency and protective effect of antioxidants. *J. Biol. Chem.* **278:** 39428–39434.
6. Christen, S., A.A. Woodall, M. K. Shigenaga, P. T. Southwell-Keely, M. W. Duncan, and B. N. Ames. 1997. gamma-Tocopherol traps mutagenic electrophiles such as NOx and complements alpha-tocopherol: physiological implications. *Proc. Natl. Acad. Sci. U S A.* **94:** 3217–3222.
7. Jiang, Q., and B. N. Ames. 2003. gamma-Tocopherol, but not alpha-tocopherol, decreases proinflammatory eicosanoids and inflammation damage in rats. *FASEB J.* **17:** 816–822.
8. Jiang, Q., J. Lykkesfeldt, M. K. Shigenaga, E. T. Shigeno, S. Christen, and B. N. Ames. 2002. gamma-Tocopherol supplementation inhibits protein nitration and ascorbate oxidation in rats with inflammation. *Free Radic. Biol. Med.* **33:** 1534–1542.
9. Jiang, Q., J. Wong, H. Fyrst, J. D. Saba, and B. N. Ames. 2004. gamma-Tocopherol or combinations of vitamin E forms induce cell death in human prostate cancer cells by interrupting sphingolipid synthesis. *Proc. Natl. Acad. Sci. USA.* **101:** 17825–17830.
10. McCormick, C. C., and R. S. Parker. 2004. The cytotoxicity of vitamin E is both vitamer- and cell-specific and involves a selectable trait. *J. Nutr.* **134:** 3335–3342.
11. Sontag, T. J., and R. S. Parker. 2002. Cytochrome P450 omega-hydroxylase pathway of tocopherol catabolism. Novel mechanism of regulation of vitamin E status. *J. Biol. Chem.* **277:** 25290–25296.
12. Swanson, J. E., R. N. Ben, G. W. Burton, and R. S. Parker. 1999. Urinary excretion of 2,7, 8-trimethyl-2-(beta-carboxyethyl)-6-hydroxychroman is a major route of elimination of gamma-tocopherol in humans. *J. Lipid Res.* **40:** 665–671.
13. Schönfeld, A., M. Schultz, M. Petrizka, and B. Gassmann. 1993. A novel metabolite of RRR-alpha-tocopherol in human urine. *Nahrung.* **37:** 498–500.
14. Wechter, W. J., D. Kantoci, E. D. Murray, Jr., D. C. D'Amico, M. E. Jung, and W. H. Wang. 1996. A new endogenous natriuretic factor: LLU-alpha. *Proc. Natl. Acad. Sci. USA.* **93:** 6002–6007.
15. Sontag, T. J., and R. S. Parker. 2007. Influence of major structural features of tocopherols and tocotrienols on their omega-oxidation by tocopherol-omega-hydroxylase. *J. Lipid Res.* **48:** 1090–1098.
16. Bardowell, S. A., F. Duan, D. Manor, J. E. Swanson, and R. S. Parker. 2012. Disruption of mouse cytochrome p450 4f14 (cyp4f14 gene) causes severe perturbations in vitamin E metabolism. *J. Biol. Chem.* **287:** 26077–26086.
17. Gu, J., Y. Weng, Q. Y. Zhang, H. Cui, M. Behr, L. Wu, W. Yang, L. Zhang, and X. Ding. 2003. Liver-specific deletion of the NADPH-cytochrome P450 reductase gene: impact on plasma cholesterol homeostasis and the function and regulation of microsomal cytochrome P450 and heme oxygenase. *J. Biol. Chem.* **278:** 25895–25901.
18. Henderson, C. J., D. M. Otto, D. Carrie, M. A. Magnuson, A. W. McLaren, I. Rosewell, and C. R. Wolf. 2003. Inactivation of the hepatic cytochrome P450 system by conditional deletion of hepatic cytochrome P450 reductase. *J. Biol. Chem.* **278:** 13480–13486.
19. Shin, H. C., H. R. Kim, H. J. Cho, H. Yi, S. M. Cho, D. G. Lee, A. M. Abd El-Aty, J. S. Kim, D. Sun, and G. L. Amidon. 2009. Comparative gene expression of intestinal metabolizing enzymes. *Biopharm. Drug Dispos.* **30:** 411–421.
20. D'Agostino, J., X. Ding, P. Zhang, K. Jia, C. Fang, Y. Zhu, D. C. Spink, and Q. Y. Zhang. 2012. Potential biological functions of cytochrome P450 reductase-dependent enzymes in small intestine: novel link to expression of major histocompatibility complex class II genes. *J. Biol. Chem.* **287:** 17777–17788.
21. Zhao, Y., M. J. Lee, C. Cheung, J. H. Ju, Y. K. Chen, B. Liu, L. Q. Hu, and C. S. Yang. 2010. Analysis of multiple metabolites of tocopherols and tocotrienols in mice and humans. *J. Agric. Food Chem.* **58:** 4844–4852.